THE JOURNAL OF PHYSICAL CHEMISTRY C

ARTICLE

pubs.acs.org/JPCC

Observation of Inverted Regime Electron Transfer in CdSe/ZnS QDs from pH-Sensitive Single-Particle and Ensemble Fluorescence Measurements

H. C. Ko,[†,‡] C. T. Yuan,[‡] S. H. Lin,[§] and Jau Tang*[,‡]

[†]Molecular Science and Technology Program, Taiwan International Graduate Program, Institute of Atomic and Molecular Sciences, Academia Sinica, Taipei, Taiwan 11529, and Department of Chemistry, National Tsing Hua University, Hsinchu, Taiwan 30013

[‡]Research Center for Applied Sciences, Academia Sinica, Taipei, Taiwan 11529

[§]Institute of Applied Chemistry, National Chiao-Tung University, Hsinchu, Taiwan 30013

ABSTRACT: In this report, we investigated the pH dependence of the photoluminescence of CdSe/ZnS quantum dots (QDs). We present experimental results and theoretical analysis of both the blinking behavior of single-QDs as well as the fluorescence intensity time trace from an ensemble of QDs in agarose gel fibers at different pH environments. Such a combined approach of confined QDs by single-particle and ensemble measurements has not been used previously. This study allows us to elucidate the electron transfer processes from the light state to the dark state. The observed increase in both the activation energy for the charge transfer and the free energy gap between the light and the dark states at an increased concentration of H^+ ions supported the Marcus inverted-regime electron transfer.

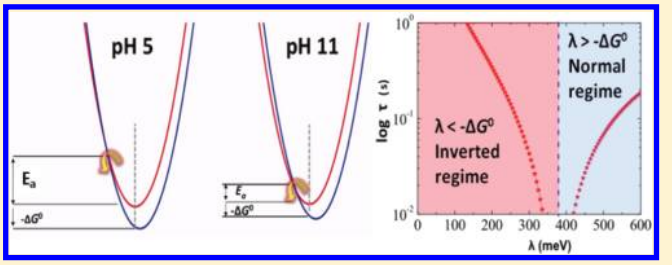

I. INTRODUCTION

Low-cost, water-soluble colloidal semiconductor quantum dots (QDs) have attracted much attention due to their excellent fluorescence properties, such as a large absorption cross section, a high quantum yield, better photostability and size-dependent optical properties.[1−3] Also, one could modify the photoluminescence quantum yield of QDs by dissolving them in solutions and attaching appropriate ligands to their surface.[4] Therefore, one major potential application of QDs is fluorescence labeling in biological system studies.[5,6] Moreover, due to the large surface to volume ratio for colloidal QDs, some photophysical properties involving energy or charge transfer are very sensitive to their surrounding environment.[7−10] Colloidal QDs have been widely used in biological systems, but most often involving an ensemble of QDs. To study QDs on a single-particle level, it is easier to embed QDs in a solid or matrix[11] to avoid complication due to diffusive processes of QDs in natural aqueous solution environments.

Several studies have shown that the optical properties of QDs are highly dependent on physical and chemical environmental parameters such as pH,[12,13] temperature,[14,15] and electric field,[16] making QDs favorable candidates for sensor applications. Recently, many types of ion-sensitive sensors based on optical detection were developed.[17,18] For example, colloidal QDs could have complex interactions with the solvent in natural solution. When some cations (Ag^+, Cu^{2+}, and K^+) are dissolved in a colloidal QD solution, fluorescence could be quenched via energy transfer from excited QDs to the cations.[18−22] Thus, the existence of such cations can be detected by monitoring ensemble fluorescence intensity. Therefore, an understanding of the photophysical properties of colloidal QDs in aqueous solution, even down to single-QD levels, is relevant to the development of potential applications in biological labeling, sensing, and single-particle tracking.[23]

The pH sensing is an important assay for biological applications. Previously, the plasmon resonance frequency of metal nanoparticles has been exploited as a means to measure the pH value.[24,25] However, these methods suffer from low sensitivity due to their broad extinction spectrum. On the other hand, the fluorescence intensity of ensemble colloidal QDs are sensitive to solvent pH values; thus they have been utilized as pH sensors.[12,13] Generally speaking, QDs are highly sensitive to pH, and as the pH increases, a small red shift and an increase in fluorescence intensity could be observed.[26] However, the fluorescence intensity could also be affected by many other factors, such as background fluorescence and light scattering, especially in complex biological environments. In addition, as of today, several QD-based pH sensors using the intensity-based response[13,26−28] or fluorescence resonance energy transfer (FRET)-based QD pH-sensing schemes[29−31] have been performed at ensemble levels. Those experiments require several milliliters of a QDs solution to achieve a sufficient signal-to-noise ratio. This requirement leads to the generation of large amounts of colloidal QDs, which needs to be disposed of, and the toxicity of these colloidal QDs has yet to be determined.

The fluorescence properties of colloidal QDs have been intensively investigated down to single-QD levels, revealing

Received: February 2, 2011
Revised: June 3, 2011
Published: June 22, 2011

some unique phenomena including fluorescence blinking. At the first glance, blinking behavior seems to be a detrimental effect that could be suppressed by reducing quantum confinement to inhibit Auger recombination. Several other methods have also been proposed to suppress blinking, such as modified synthesis,[32] increasing the shell thickness of QDs,[33−35] surface passivation with appropriate molecules,[36−38] surface plasmon effects via coupling to metallic nanoparticles,[39−41] and blocking electron transfer from the light state to dark state.[42,43] In a recent study, single QDs with a gradient in the alloyed composition from the core to the surface have been found to be nonblinking.[44] Indeed, fluorescence blinking is a disadvantageous feature for colloidal QDs as single-photon light sources. Nevertheless, such blinking behavior is sensitive to variations in the ambient surroundings, thus could provide useful information about local environments for QDs as pH sensors.

In this work, single colloidal QDs encapsulated in agarose gel in a natural aqueous solution were employed to probe solvent pH values. In this case, pH values can be sensed on the basis of single-QD blinking statistics, which suggests a coupling role of H^+ ions in the underlying mechanism of the QD's photophysical properties. Finally, we will offer explanations regarding the effects of the pH environment on the blinking behavior. We believe that such QD-based sensing has significant applications for future chemical and biological assays.

II. EXPERIMENTAL SECTION

Colloidal CdSe/ZnS nontargeted, PEG-coated QDs emitting at 565 nm were purchased from Invitrogen. To investigate the effects of acid or base on QD fluorescence, agarose gel (Sigma-Aldrich) solutions with different pH values were mixed with the QD solution and then spin-coated on a glass substrate. The experiments were conducted using a far-field laser scanning confocal microscope (MicroTime 200, PicoQuant). In our system, the mean separation between QDs was larger than the excitation laser spot, thus allowing for the monitoring of individual QDs. The sample was excited with a pulsed diode laser (PDL 800-D) operating at 467 nm (~380 W/cm^2) through a × 100 objective (Olympus, N.A. = 1.4).

The fluorescence was collected by the same objective and guided to a confocal pinhole (~50 μm) to block the out-of-focus light. Through the pinhole, the fluorescence was split by a beam splitter cube into two beams, then filtered through a 565/40 band-pass filter (D565/40; Chroma Tech), and detected by a pair of single-photon avalanche photon diodes (SPCM-AQR-14; PerkinElmer). Fluorescence images were first obtained by raster scanning with a piezo-driven nanopositioning and scanning system (E-710; Physik Instrument). After the images of single QDs were obtained, each particle was moved consecutively to the focal point of the objective to record the time evolution of the fluorescence intensity. For the ensemble measurements the fluorescence intensity time profile was measured with a JASCO FP-6300 fluorescence spectrophotometer at room temperature. The sample was excited by a xenon lamp operating at 467 nm with the excitation intensity at ~25 mW/cm^2.

III. THEORETICAL SECTION

Photoluminescence of semiconducting nanocrystals has been investigated on a single particle level as well as in an ensemble system,[45] and there are subtle differences between them. For single particle case, single QDs fluorescence intensity histogram

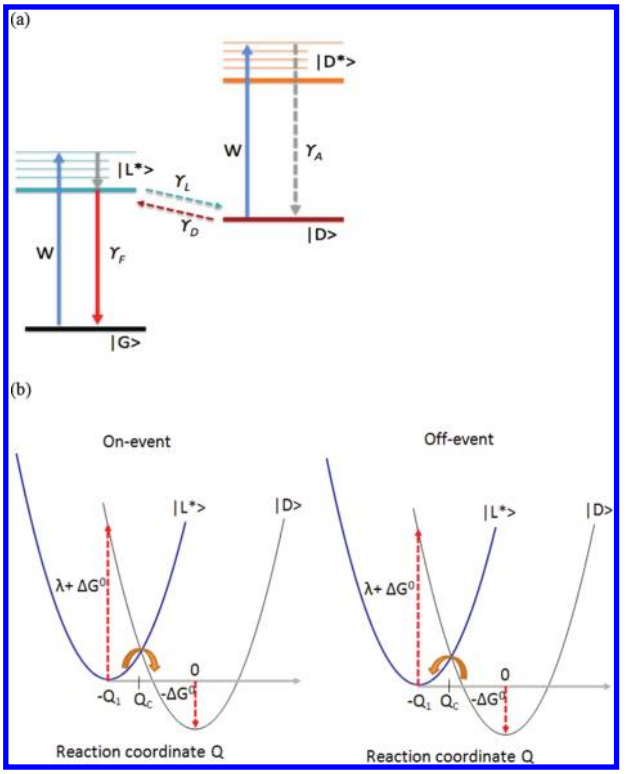

Figure 1. (a) Schematic diagram of DCET model. (b) Diffusion on the parabolic potential surfaces for light sate $|L^*\rangle$ and dark state $|D\rangle$.

shows binary stochastic jumps between two levels, "on" and "off". The "off" state appears dark due to fast nonradiative Auger process. Once could determine from the fluorescence blinking histogram the duration of "on" or "off" periods to calculate the probability distribution $P_{on}(t)$ and $P_{off}(t)$ for the "on" or "off" events. On the other hand, in the ensemble experiment, the fluorescence intensity time profile represents collection of fluorescent photons emitted simultaneously from a huge number of QDs, and QDs in such an ensemble measurement are indistinguishable. Therefore, the ensemble-averaged fluorescence time profile $\langle I(t)\rangle$ represents the sum of all fluorescence histograms from each individual QDs after the continuous laser excitation is turned on. For that reason, to calculate $\langle I(t)\rangle$ one needs to consider coupled rate equations including both forward and reverse charge transfer reactions, whereas to describe either $P_{on}(t)$ or $P_{off}(t)$ of a single QD, which is a distinguishable particle, one only needs to consider the forward or reverse rate equation.[46]

A. Intermittency of Single QDs Based on the Diffusion-Controlled Electron Transfer Model. The diffusion-controlled electron transfer (DCET) model[46−48] assumed that fluctuations occurred in energy configuration space, represented by a one-dimensional reaction coordinate. The schematic diagram for the model is shown in Figure 1a, where W is the photoexcitation rate, γ_F is the fluorescence decay rate, and γ_L and γ_D are the forward and backward transition rate between $|L^*\rangle$ and $|D\rangle$, respectively. There are two neutral states (ground state $|G\rangle$ and excited light state $|L^*\rangle$) and two charge-separated states. $|D\rangle$ represents a charge-separated state with a positively charged hole in the core of a QD and a counter-charge trapped on some surface states,[49,50] which are below the edge of the quasi-conduction band or just above the edge of the quasi-valence band. When an additional exciton is generated in the state $|D\rangle$ upon further photoexcitation

to the state $|D^*\rangle$, instead of emitting a fluorescent photon, the excitonic energy is quickly transferred to the mobile hole in the core via the radiationless Auger relaxation process. Therefore, as a consequence of fast Auger relaxation the state $|D\rangle$ appears dark. The transitions between $|L^*\rangle$ and $|G\rangle$ is the bottleneck process related to fluorescence intermittency.

As illustrated in Figure 1b, the potentials for $|L^*\rangle$ and $|D\rangle$ are defined as $U_1(Q) = \kappa_E(Q + Q_1)^2/2$ and $U_2(Q) = \Delta G^0 + \kappa_E Q^2/2$, where ΔG^0 is the free-energy gap between $|L^*\rangle$ and $|D\rangle$, κ_E is the force constant, and $\lambda = \kappa_E Q_1^2/2$ is reorganization energy for the electron transfer. The energy-level crossing occurs at $Q_c = (\Delta G^0 - \lambda)/(2\kappa_E\lambda)^{1/2}$.

The probability distribution for a QD to stay in the light state $|L^*\rangle$ or the dark state $|D\rangle$ can be calculated. The time evolution of population distribution $\rho_1(Q,t)$ on potential $U_1(Q)$ and a sink at Q_c as below:[48]

$$\frac{\partial}{\partial t}\rho_1(Q,t) = \frac{1}{\tau}\left(\Delta^2\frac{\partial^2}{\partial Q^2} + \left(1 + (Q + Q_1)\frac{\partial}{\partial Q}\right)\right)\rho_1(Q,t) - \frac{2\pi|V_{12}|^2}{\hbar}\delta(U_1(Q) - U_2(Q))\,\rho_1(Q,t) \quad (1)$$

where $\Delta^2/\tau \equiv D$ is the diffusion coefficient, V_{12} represents the electronic coupling between $|L^*\rangle$ and $|D\rangle$, and the initial condition is defined as $\rho_1(Q,0) = \delta(Q - Q_c)$. The above equation represents the rate equation involving nonadiabatic electron transfer reactions for the population in the light state. This equation describes a 1-D diffusion-controlled electron transfer reaction on parabolic free-energy potentials with a reaction sink at their intersection.[48] By using the Green function method, we can solve the blinking statistics $P_{on}(t)$ for the on-events. According to the previous studies,[46−48] the waiting time distribution for the on-events is given by

$$P(t) \propto t^{-m}e^{-\Gamma t} \quad (2)$$

where

$$\Gamma\tau \equiv \frac{E_a}{2k_BT} \qquad E_a \equiv \frac{(\lambda + \Delta G^0)^2}{4\lambda} \quad (3)$$

The exponent m for the inverse power law equals to 3/2 for normal diffusion and could take a different value for anomalous diffusion.[47] According to the above equation, $P_{on}(t)$ follows a power law with an exponential bending tail, whereas the bending tail factor Γ, as shown in eq 3, is related to the activation energy E_a for the forward electron transfer reaction. Such a relationship will be used later in analyzing experimental blinking statistic data of single QDs.

B. Ensemble-Averaged Fluorescence Intensity. To calculate the ensemble-averaged fluorescence intensity decay, one needs to solve the coupled rate equations involving both forward and backward transitions between the light state and the dark state. According to our previous work,[48] the normalized fluorescence intensity in the Laplace transform domain of s is given by

$$\bar{I}(s) \equiv \int_{-\infty}^{\infty} dQ\,\overline{\rho_1}(Q,s) = \frac{\zeta_1}{s}\left\{1 - \frac{\gamma_1}{s[1 + \bar{g}_1(s) + \bar{g}_2(s)]}\right\} \quad (4)$$

where the Laplace transform of the Greens function is defined as $\bar{g}_k(s) \equiv A_k\overline{G_k}(Q_c,Q_c;s)$ and $A_k = (2\pi|V_k|^2/\hbar)|\partial(U_1(Q) - U_2(Q))/\partial Q|_{Q=Q_c}$.

Although the exact expression could not be obtained for eq 4, it could be expressed approximately by[48]

$$I(t) = I_{eq} + (1 - I_{eq})\exp(-(t/T_0)^{\alpha}) \quad (5)$$

where

$$I_{eq} \equiv \frac{1}{[1 + \zeta\exp(-\Delta G^0/k_BT]} \quad (6)$$

and $\varsigma \equiv W/(W + \gamma_F) \sim W/\gamma_F$, W is the photoexcitation rate, and γ_F is the fluorescence decay rate. From the above equation one could relate the equilibrium fluorescence intensity I_{eq} at long time to the free energy gap ΔG^0 between $|L^*\rangle$ and $|D\rangle$. Such a relationship will be used in the next section to analyze our ensemble experimental data of QDs.

IV. RESULTS AND DISCUSSION

Many theoretical models have been proposed to explain the blinking phenomenon of single QDs, including diffusion-controlled electron transfer (DCET) model,[47,48] charge tunneling model,[51] and some other models.[52] Here, the framework of the DCET model was considered to interpret our experimental results. Figure 2a shows the on-time distribution $P_{on}(t)$ in log−log scale of single QDs at different pH values (5, 7, 9, and 11). In general, the choices of binning time and threshold could affect the power-law distributions of on-times.[53] To determine exactly the on-time distribution, a bin time of 10 ms and a threshold of about one-third of the highest peak of fluorescence intensity histogram were used. Here, $P_{on}(t)$ exhibits an inverse power-law distribution at shorter times but then deviates from this distribution at longer times, exhibiting an exponential bending tail. The distribution was fitted using $P(t) \sim ct^{-m}\exp(-\Gamma t)$ of eq 2, where c is an unimportant scaling constant, m is the power-law exponent, and Γ is the bending rate, which is related to the activation energy of the electron transfer.[46−48] In this case, m is typically around 1.5. In general, a trend was observed with shorter "on" events at lower pH values. Furthermore, similar to the previous report,[54] the bending rate Γ increases as the pH value decreases (Figure 2b). According to the DCET model,[46−48] Γ increases with the activation energy for the electron transfer from the light sate to the dark state. Therefore, our data demonstrate that the activation energy also increases with the H^+ ion concentration.

With measured dependence of the bending rate Γ of the blinking statistics on the H^+ ion concentration to precisely determine the activation energy based on eq 3 one needs to know the diffusion correlation time constant τ. Because the spectral diffusion is sensitive to light excitation, and $1/\tau$ is related to the ratio ζ of the photoexcitation rate W and the fluorescent decay rate γ_F. The magnitude of W is related to the excitation intensity and the photoabsorption cross section of QDs. The CdSe/ZnS QDs used in our experiments has a peak emission at 565 nm, and the radius was estimated to be around 2.1 nm.[55] Due to the absorption cross section σ is directly proportional to the volume of QDs,[56] we obtained an estimate of $\sigma \sim 7.0 \times 10^{-16}$ cm^{-2} and $W \sim 41.2$. Figure 3 shows the decay profiles of single QDs on a glass substrate in comparison with QDs embedded in 1% agarose gel with different pH values from 3 to 11. The average fluorescence lifetime of QDs embedded in pH 3 agarose gel is about 13 ns, which is faster than that of QDs on glass (26 ns). As shown in Figure 4, we observed that $\Gamma\gamma_F/W$ increases as the pH value decreases. According to eq 3, the activation energy is proportional to the bending rate Γ

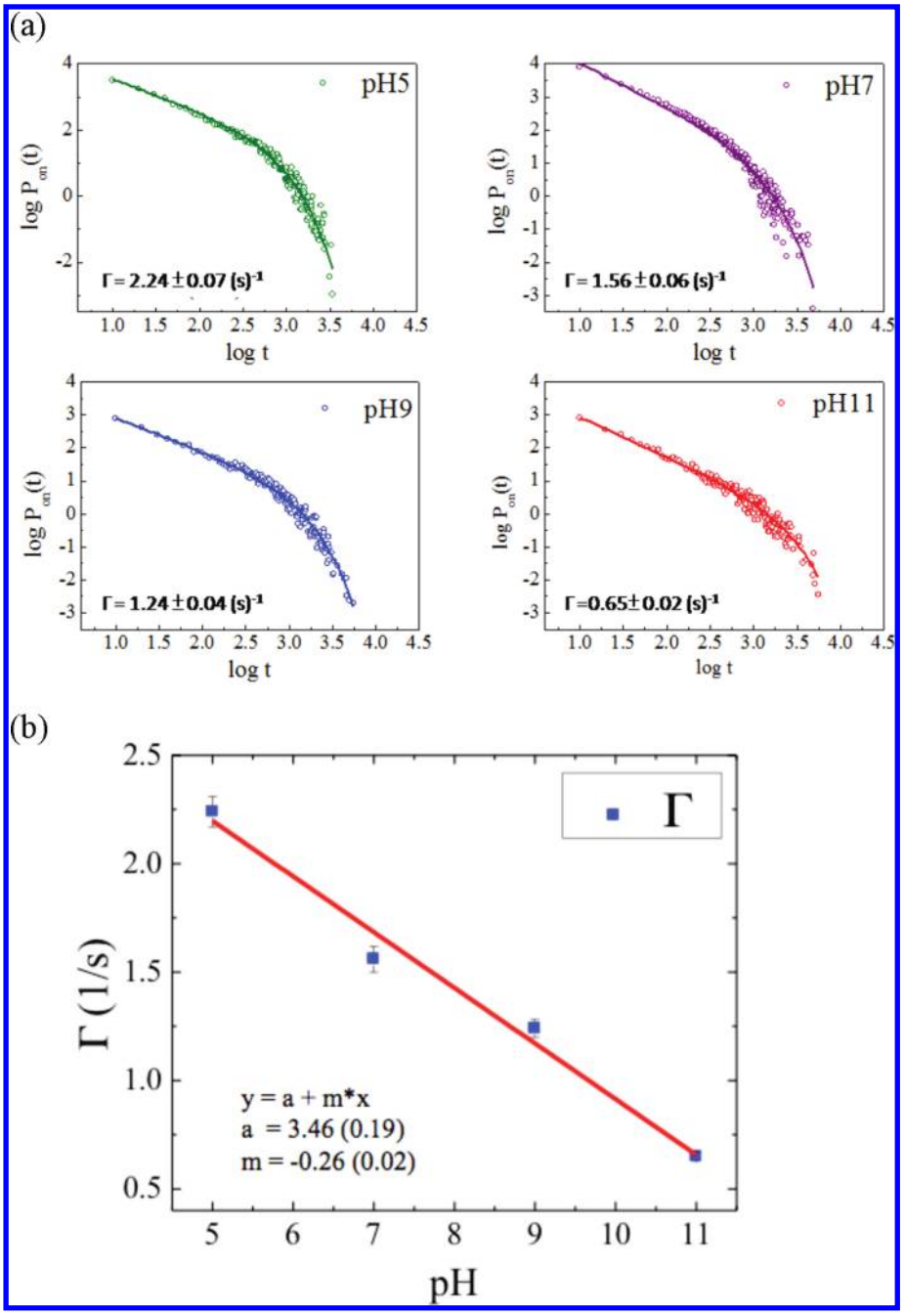

Figure 2. (a) Log−log plot of the on-time blinking statistics of single QDs in pH 5, 7, 9, and 11 gels, respectively. The time scale is milliseconds. (b) Plot of the fitted exponential bending rate vs the pH value, based on the on-event waiting time distribution curves at four pH values.

and the diffusion correlation time constant τ, and $1/\tau$ depends on the ratio of the photoexcitation rate W and the fluorescence decay rate γ_F. The linear relationship of $\Gamma\gamma_F/W$ and pH indicates that the activation energy also linearly depends on the H^+ ion concentration. All the relevant parameters are listed in Table 1.

Unlike the single-particle case, which exhibits an inverse power law for the blinking statistics, the time trace of the fluorescence intensity for an ensemble of QDs exhibits a quasi-stretched exponential decay. There exists a relationship between the single-particle and ensemble fluorescence measurements of QDs.[46] Immobilization of QDs in agarose gel are necessary to avoid complication from spatial diffusion of QDs while collecting the time trace of fluorescence from ensemble measurements extending from 1 s to 10^4 s. Figure 5a shows intensity time traces from QDs for different pH values (i.e., 4, 5, and 6) with a fit using a stretched exponential of eq 5.[46] The stretched exponential fit with three parameters T_o, α, and I_{eq} is a convenient approximate representation of the overall decaying feature of $I(t)$. Furthermore, as shown in Figure 5b, we observed a decrease in $\ln(1/I_{eq} - 1)$ as the number of H^+ ions increases. From eq 6 one has $\ln(1/I_{eq} - 1)$, or equivalently, $\ln(W/\gamma_F) - \Delta G^0/k_BT$; its linear dependence on pH indicates a linear relationship between the free energy gap between the light state and the dark state, ΔG^0, and pH. Our experimental results indicate that the H^+ ion distribution near the

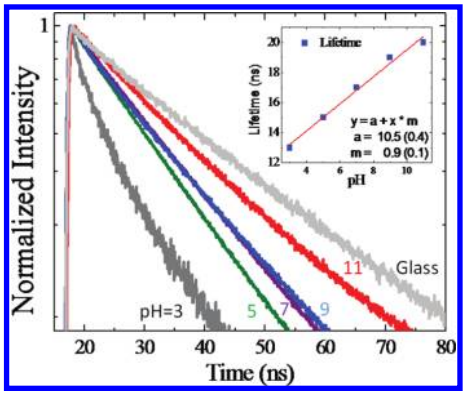

Figure 3. Fluorescence decay profiles for single QDs on a glass substrate and embedded in pH 3−11 and 1% agarose gel. The inset shows the dependence of the fitted decay time constant on pH.

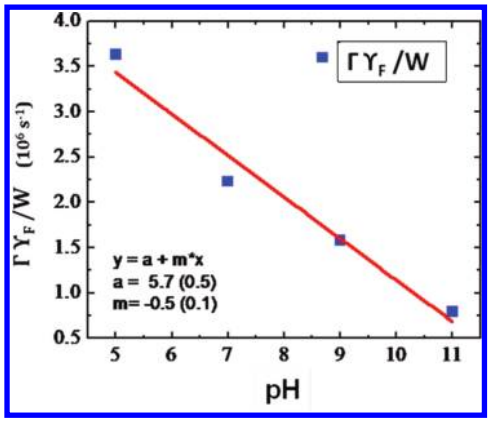

Figure 4. Plot of $\Gamma\gamma_0/W$ vs the pH value. The linear dependence on pH indicates a linear relationship between the activation energy E_a and pH.

Table 1. Measured Bending Rate Γ of the Blinking Statistics and the Fluorescence Decay Rate γ_F at Different pH Values

pH	Γ (s^{-1})	γ_F (s^{-1})	$\Gamma\gamma_F/W$ (10^6 s^{-1})
5	2.24	6.67×10^7	3.63
7	1.56	5.88×10^7	2.23
9	1.24	5.26×10^7	1.58
11	0.65	5.00×10^7	0.79

QD surface could stabilize the dark state to lower its free energy, resulting in an increase in the free energy gap between the light state and dark state. A list of the extracted free energy gap at different pH values is given in Table 2.

On the basis of the Marcus theory, the rate of electron transfer would decrease with an increase in the free energy ΔG^0 in the normal regime, but it would increase in the inverted region. The inverted region occurs when $-\Delta G^0$ is greater than the reorganization energy λ. Figure 6 shows the free energy curves for the light and dark states in the Marcus inverted regime. In this diagram ΔG^0 is the free energy gap difference between the light state $|L^*\rangle$ on the left and the dark state on the right $|D\rangle$, E_a is the activation energy, and λ is the reorganization energy. According to eq 3 the bending rate (Γ) is related the activation energy by $\Gamma\tau \equiv E_a/2k_BT$, where $E_a \equiv (\lambda + \Delta G^0)^2/4\lambda$, τ is the diffusion correlation time constant, and k_B is Boltzmann's constant.[47] When $-\Delta G^0$ is much larger than λ, a large $-\Delta G^0$ value leads to

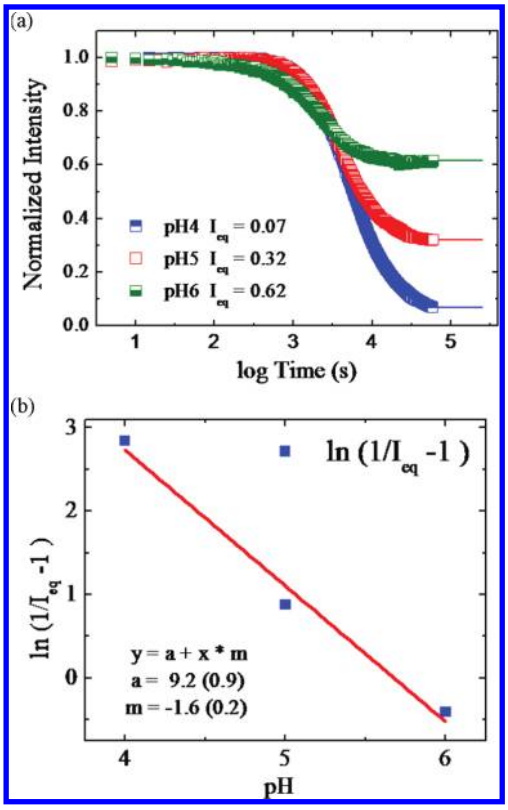

Figure 5. (a) Log-linear plot of the normalized $I(t)$ (dot curves) for an ensemble of QDs and the fitted solid curves using a stretched exponential $I_{eq} + (1 - I_{eq}) \exp[-(t/T_o)^{\alpha}]$, where I_{eq} is the asymptotic value at equilibrium. (b) Plot of $\ln(1/I_{eq} - 1)$ vs the pH value. The linear dependence on pH indicates a linear relationship between ΔG^0 and pH.

Table 2. Measured Fluorescence Intensity Asymptote I_{eq} and the Estimated Free Energy Gap ΔG^0 at Different pH Values

pH	I_{eq}	ζ	ΔG^0 (meV)
4	0.07	5.8×10^{-7}	−424
5	0.32	6.2×10^{-7}	−376
6	0.62	6.6×10^{-7}	−344

an increase in Γ, a greater bending rate. Recently, Scholes et al.[57] reported that electron transfer reactions from the QD with a core of CdSe to its shell surface states in CdTe states occur in the Marcus inverted regime, due to $\lambda < -\Delta G^0$. They observed a very small reorganization energy $\lambda \sim 20$ meV compared with $\Delta G^0 \sim -170$ meV for the photoinduced electron transfer. Majima and co-workers[58] demonstrated, from single-particle QD measurements, that the reorganization energy for the electron transfer within the CdSe/ZnS-PI in nonpolar solvents is around 280 meV, which is smaller than the free energy gap $\Delta G^0 \sim -750$ meV, and the Γ value increased with a decreasing polarity of the solvent. Therefore, the Marcus inverted regime could occur in very exothermic heterogeneous electron transfer reactions.

By analyzing the on-time distribution $P_{on}(t)$ of single QDs, we observed that the bending rate (Γ) increases with the H^+ ion concentration. According to the DCET model,[46−48] Γ is directly proportional to the activation energy for the electron transfer from the light state to the dark state. Our data demonstrate that the activation energy increases with the H^+ ion concentration.

dx.doi.org/10.1021/jp203587x |J. Phys. Chem. C 2011, 115, 13977–13984

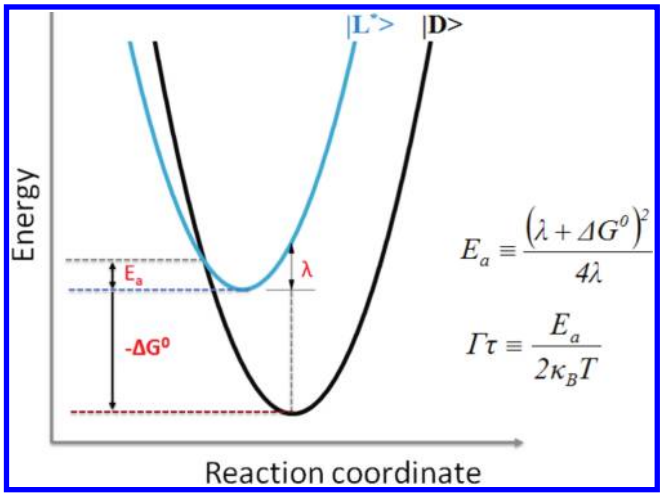

Figure 6. Free energy potentials for the light and the dark states involving the inverted regime electron transfer.

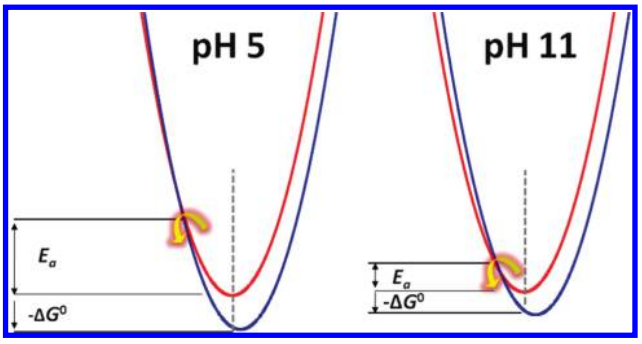

Figure 7. DCET model describing the effects of pH (H^+ ions) on the free energy gap, the activation energy that controls the bending tail for the blinking statistics in the Marcus inverted regime.

From our ensemble experimental results, the fluorescence intensity time trace of QDs is found to display increasing dependence of the value of $\ln(1/I_{eq} - 1)$ on the H^+ ion concentration, which affects the free energy gap between the light and dark states. Here, we used PEG-coated QDs for the investigation of the pH effects on the fluorescence properties of QDs. Because PEG is neutral, nonvolatile, and insensitive to pH,[59] the PEG can cause separation to protect the shell of QDs from outside environment.[60] Therefore, we believed that at pH 5 the damages on the ligand (PEG) and the shell is minor. The experimental results clearly indicated that the H^+ ion distribution near the QD surface could stabilize the dark state to lower its free energy, resulting in an increase in the free energy gap between the light state and dark state. Thus, H^+ ions surrounding the QDs might play an important role in controlling their charge transfer and blinking behavior. The H^+ ions surrounding the QDs could cause the energy of $|D\rangle$ to shift downward with respect to that of $|L^*\rangle$. Consequently, it would result in increased activation energy and a larger free energy gap, and these scenarios would occur only in the Marcus inverted regime. In Figure 7, the effects of pH (H^+ ion) on the activation energy and free energy gap in the inverted regime according are illustrated according to the DCET model.

According to eq 3, the activation energy E_a is related to Γ by $E_a = 2k_B T\Gamma\tau$. Although we could measure Γ for QDs from the exponential bending tail of the blinking statistics at a different

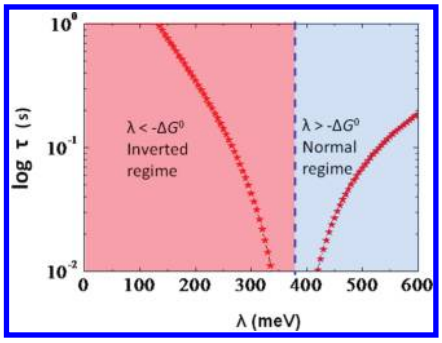

Figure 8. Semilog plot of the diffusion correlation time τ versus the reorganization energy λ based on eq 3, $\tau = (\lambda + \Delta G^0)^2/8k_B T\lambda\Gamma$, where $\Gamma = 2.24\ s^{-1}$ and the free energy gap $\Delta G^0 = -376$ meV at pH 5. The vertical line represents the activationless regime with $\lambda + \Delta G^0 = 0$ exactly. To the left of the dotted line is the inverted regime with $\lambda < -\Delta G^0$ and to the right is the normal regime with $\lambda > -\Delta G^0$.

pH, the activation energy could not be determined without knowing the value for the diffusion correlation time constant τ. This time constant could be determined from an analysis[48] of spectral diffusion measurements for single QDs, and its value is sensitive to the excitation intensity, the size of QD, and temperature. In the work we reported the observed dependence of Γ vs pH, but our lab is not equipped presently for spectral diffusion measurements to allow us to quantitatively determine the activation energy. Based on a crude estimate, with τ on the order of 1 s, with measured values of $\Gamma \sim 2\ s^{-1}$ from Figure 2, it is a reasonable guess of E_a to be on the order of 100 meV. With $\Gamma = 2.24\ s^{-1}$ and the free energy gap $\Delta G^0 = -376$ meV at pH 5, the relationship in eq 3 between the diffusion correlation time τ and the reorganization energy λ is illustrated by Figure 8. There are two regimes, the inverted vs the normal regimes, to the left and right of the vertical dot line representing the activationless regime where $\lambda + \Delta G^0 = 0$ exactly. From such a plot, one can determine the value of λ once τ is known. The determination of τ requires future measurements of spectral diffusion for each single QD.[61−63] Because our experimental results support the inverted regime electron transfer, we expect that the organization energy λ should be much smaller than the free energy gap. Such observation and the estimates of ΔG^0 and λ seem to be in line with the previous report by Scholes et al.[57]

V. CONCLUSIONS

In conclusion, unlike previous studies by others that emphasized either an ensemble system or a single-QD system, we performed in this work both single-particle and ensemble QDs fluorescence measurements and analyzed these data to provide a clearer physical picture of how pH environment affects the electron transfer between the light and dark states of QDs. Moreover, we reported the finding of the unusual Marcus inverted regime for the electron transfer from the light state to the dark state. Such a situation often occurs when the reorganization energy for the charge transfer is much smaller than the free energy gap between the reactant and the product states. This conclusion was drawn on the basis of our systematical studies on the blinking behavior of single QDs and the fluorescence time trace from ensemble QDs in different pH environments. Single colloidal QDs encapsulated in agarose gel in a natural aqueous solution were used to probe the solvent pH value.

Generally speaking, the interaction of H^+ ions with QDs to induce fluorescence quenching can be attributed to nonradiative recombination pathways and electron transfer processes. We offered explanations regarding the effects of the pH environment on the blinking behavior. According to the DCET model, the exponential bending rate is expected to increase with the activation energy of the electron transfer from the light state to the dark state. The H^+ ion distribution near the QD surface could stabilize the dark state to lower its free energy, resulting in an increase of the activation energy and the observed increase in the free energy gap. Such an increase of the activation energy and a simultaneous increase in the free energy gap would occur only in the unusual Marcus inverted regime. Such a scenario indicates small reorganization energy for this system. Other than reaching such an important qualitative result, we have also determined the free energy gap at different pH values from the ensemble measurements of the fluorescence intensity time profiles. We have also given an estimate for the reorganization energy. The observation of the pH dependence for the fluorescence blinking, fluorescence lifetime for single QDs and the fluorescence intensity time profile indicates that such a QD sensing scheme could offer potentially significant applications for chemical and biological assays.

AUTHOR INFORMATION

Corresponding Author

*E-mail: jautang@gate.sinica.edu.tw.

ACKNOWLEDGMENT

J.T. thanks the support of National Science Council of Taiwan under the program No. 99-2113-M-001-023-MY3 and the Academia Sinica.

REFERENCES

(1) Zamir, E.; Lommerse, P. H. M.; Kinkhabwala, A.; Grecco, H. E.; Bastiaens, P. I. H. *Nat. Methods* **2010**, *7*, 295–298.
(2) Norris, D. J.; Sacra, A.; Murray, C. B.; Bawendi, M. G. *Phys. Rev. Lett.* **1994**, *72*, 2612–2615.
(3) Sha, L.; Kai, Z.; Jui-Ming, Y.; Liwei, L.; Haw, Y. *Nano Lett.* **2007**, *7*, 3102–3105.
(4) Knowles, K. E.; Tice, D. B.; McArthur, E. A.; Solomon, G. C.; Weiss, E. A. *J. Am. Chem. Soc.* **2010**, *132*, 1041–1050.
(5) Medintz, I. L.; Uyeda, H. T.; Goldman, E. R.; Mattoussi, H. *Nat. Mater.* **2005**, *4*, 435–446.
(6) Parak, W. J.; Pellegrino, T.; Plank, C. *Nanotechnology* **2005**, *16*, R9–R25.
(7) Murphy, C. J. *Anal. Chem.* **2002**, *74*, 520a–526a.
(8) Jones, M.; Lo, S. S.; Scholes, G. D. *Proc. Natl. Acad. Sci. U. S. A.* **2009**, *106*, 3011–3106.
(9) Jin, S. Y.; Hsiang, J. C.; Zhu, H. M.; Song, N. H.; Dickson, R. M.; Lian, T. Q. *Chem. Sci* **2010**, *1*, 519–526.
(10) Krooswyk, J. D.; Tyrakowski, C. M.; Snee, P. T. *J. Phys. Chem. C* **2010**, *114*, 21348–21352.
(11) Yuan, C. T.; Yu, P.; Ko, H. C.; Huang, J.; Tang, J. *ACS Nano* **2009**, *3*, 3051–3056.
(12) Gao, X. H.; Chan, W. C. W.; Nie, S. M. *J. Biomed. Opt.* **2002**, *7*, 532–537.
(13) Tomasulo, M.; Yildiz, I.; Raymo, F. M. *J. Phys. Chem. B* **2006**, *110*, 3853–3855.
(14) Biju, V.; Makita, Y.; Sonoda, A.; Yokoyama, H.; Baba, Y.; Ishikawa, M. *J. Phys. Chem. B* **2005**, *109*, 13899–13905.
(15) Walker, G. W.; Sundar, V. C.; Rudzinski, C. M.; Wun, A. W.; Bawendi, M. G.; Nocera, D. G. *Appl. Phys. Lett.* **2003**, *83*, 3555–3557.
(16) Muller, J.; Lupton, J. M.; Lagoudakis, P. G.; Schindler, F.; Koeppe, R.; Rogach, A. L.; Feldmann, J.; Talapin, D. V.; Weller, H. *Nano Lett.* **2005**, *5*, 2044–2049.
(17) Zhang, F.; Ali, Z.; Amin, F.; Feltz, A.; Oheim, M.; Parak, W. J. *Chemphyschem* **2010**, *11*, 730–735.
(18) Liang, J. G.; Ai, X. P.; He, Z. K.; Pang, D. W. *Analyst* **2004**, *129*, 619–622.
(19) Gattas-Asfura, K. A.; Leblanc, R. M. *Chem. Commun.* **2003**, 2684–2685.
(20) Ruedas-Rama, M. J.; Wang, X. J.; Hall, E. A. H. *Chem. Commun.* **2007**, 1544–1546.
(21) Dong, C. Q.; Qian, H. F.; Fang, N. H.; Ren, J. C. *J. Phys. Chem. B* **2006**, *110*, 11069–11075.
(22) Xie, H. Y.; Liang, H. G.; Zhang, Z. L.; Liu, Y.; He, Z. K.; Pang, D. W. *Spectrochim. Acta Part A* **2004**, *60*, 2527–2530.
(23) Pouya, S.; Koochesfahani, M.; Snee, P.; Bawendi, M.; Nocera, D. *Exp. Fluids* **2005**, *39*, 784–786.
(24) Ni, W. H.; Chen, H. J.; Su, J.; Sun, Z. H.; Wang, J. F.; Wu, H. K. *J. Am. Chem. Soc.* **2010**, *132*, 4806–4814.
(25) Xue, C.; Mirkin, C. A. *Angew. Chem., Int. Ed.* **2007**, *46*, 2036–2038.
(26) Liu, Y. S.; Sun, Y. H.; Vernier, P. T.; Liang, C. H.; Chong, S. Y. C.; Gundersen, M. A. *J. Phys. Chem. C* **2007**, *111*, 2872–2878.
(27) Susha, A. S.; Javier, A. M.; Parak, W. J.; Rogach, A. L. *Colloids Surf., A* **2006**, *281*, 40–43.
(28) Deng, Z. T.; Zhang, Y.; Yue, J. C.; Tang, F. Q.; Wei, Q. *J. Phys. Chem. B* **2007**, *111*, 12024–12031.
(29) Snee, P. T.; Somers, R. C.; Nair, G.; Zimmer, J. P.; Bawendi, M. G.; Nocera, D. G. *J. Am. Chem. Soc.* **2006**, *128*, 13320–13321.
(30) Suzuki, M.; Husimi, Y.; Komatsu, H.; Suzuki, K.; Douglas, K. T. *J. Am. Chem. Soc.* **2008**, *130*, 5720–5725.
(31) Chen, Y.; Thakar, R.; Snee, P. T. *J. Am. Chem. Soc.* **2008**, *130*, 3744–3745.
(32) Biju, V.; Makita, Y.; Nagase, T.; Yamaoka, Y.; Yokoyama, H.; Baba, Y.; Ishikawa, M. *J. Phys. Chem. B* **2005**, *109*, 14350–14355.
(33) Mahler, B.; Spinicelli, P.; Buil, S.; Quelin, X.; Hermier, J. P.; Dubertret, B. T. *Nat. Mater.* **2008**, *7*, 659–664.
(34) Spinicelli, P.; Buil, S.; Quelin, X.; Mahler, B.; Dubertret, B.; Hermier, J. P. *Phys. Rev. Lett.* **2009**, *102*, 136801.
(35) Garcia-Santamaria, F.; Chen, Y. F.; Vela, J.; Schaller, R. D.; Hollingsworth, J. A.; Klimov, V. I. *Nano Lett.* **2009**, *9*, 3482–3488.
(36) Fomenko, V.; Nesbitt, D. J. *Nano Lett.* **2008**, *8*, 287–293.
(37) Hohng, S.; Ha, T. *J. Am. Chem. Soc.* **2004**, *126*, 1324–1325.
(38) Early, K. T.; McCarthy, K. D.; Hammer, N. I.; Odoi, M. Y.; Tangirala, R.; Emrick, T.; Barnes, M. D. *Nanotechnology* **2007**, *18*, 424027.
(39) Yuan, C. T.; Yu, P.; Tang, J. *Appl. Phys. Lett.* **2009**, *94*, 243108.
(40) Shimizu, K. T.; Woo, W. K.; Fisher, B. R.; Eisler, H. J.; Bawendi, M. G. *Phys. Rev. Lett.* **2002**, *89*, 117401.
(41) Matsumoto, Y.; Kanemoto, R.; Itoh, T.; Nakanishi, S.; Ishikawa, M.; Biju, V. *J. Phys. Chem. C* **2008**, *112*, 1345–1350.
(42) Ko, H. C.; Yuan, C. T.; Lin, S. H.; Tang, J. *Appl. Phys. Lett.* **2010**, *96*, 012104.
(43) Ko, H. C.; Yuan, C. T.; Tang, J. *Nano Rev.* **2011**, *2*, 5895.
(44) Wang, X. Y.; Ren, X. F.; Kahen, K.; Hahn, M. A.; Rajeswaran, M.; Maccagnano-Zacher, S.; Silcox, J.; Cragg, G. E.; Efros, A. L.; Krauss, T. D. *Nature* **2009**, *459*, 686–689.
(45) Chung, I. H.; Bawendi, M. G. *Phys. Rev. B* **2004**, *70*, 165304.
(46) Tang, J.; Marcus, R. A. *J. Chem. Phys.* **2005**, *123*, 204511.
(47) Tang, J.; Marcus, R. A. *Phys. Rev. Lett.* **2005**, *95*, 107401.
(48) Tang, J.; Marcus, R. A. *J. Chem. Phys.* **2005**, *123*, 054704.
(49) Williamson, A. J.; Zunger, A. *Phys. Rev. B* **2000**, *61*, 1978–1991.
(50) Franceschetti, A.; Zunger, A. *Phys. Rev. B* **2000**, *62*, R16287–R16289.
(51) Kuno, M.; Fromm, D. P.; Johnson, S. T.; Gallagher, A.; Nesbitt, D. J. *Phys. Rev. B* **2003**, *67*, 125304.
(52) Frantsuzov, P. A.; Kuno, M.; Janko, B.; Marcus, R. A. *Nat. Phys.* **2008**, *4*, 519–522.
(53) Crouch, C. H.; Sauter, O.; Wu, X.; Purcell, R.; Querner, C.; Drndic, M.; Pelton, M. *Nano Lett.* **2010**, *10*, 1692–1698.

(54) Durisic, N.; Wiseman, P. W.; Grutter, P.; Heyes, C. D. *ACS Nano* **2009**, *3*, 1167–1175.
(55) Dabbousi, B. O.; RodriguezViejo, J.; Mikulec, F. V.; Heine, J. R.; Mattoussi, H.; Ober, R.; Jensen, K. F.; Bawendi, M. G. *J. Phys. Chem. B* **1997**, *101*, 9463–9475.
(56) Lounis, B.; Bechtel, H. A.; Gerion, D.; Alivisatos, P.; Moerner, W. E. *Chem. Phys. Lett.* **2000**, *329*, 399–404.
(57) Scholes, G. D.; Jones., M.; Kumar., S. *J. Phys. Chem. C* **2007**, *111*, 13777–13785.
(58) Cui, S. C.; Tachikawa, T.; Fujitsuka, M.; Majima, T. *J. Phys. Chem. C* **2010**, *114*, 1217–1225.
(59) Hwang, S. J.; Kim, M. S.; Han, J. K.; Lee, D. S.; Kim, B. S.; Choi, E. K.; Park, H. J.; Kim, A. S. *Macromol. Res.* **2007**, *15*, 437–442.
(60) Kelf, T. A.; Sreenivasan, V. K. A.; Sun, J.; Kim, E. J.; Goldys, E. M.; Zvyagin, A. V. *Nanotechnology* **2010**, *21*, 285105.
(61) Empedocles, S. A.; Bawendi, M. G. *J. Phys. Chem. B* **1999**, *103*, 1826–1830.
(62) Tang, J.; Marcus, R. A. *J. Chin. Chem. Soc.* **2006**, *53*, 1–13.
(63) Tang, J. *J. Chem. Phys.* **2008**, *129*, 084709.